IEEE Journal of Microwaves

Received 22 February 2021; revised 13 April 2021 and 26 May 2021; accepted 26 May 2021. Date of publication 18 June 2021; date of current version 7 July 2021.

Digital Object Identifier 10.1109/JMW.2021.3084917

A Compact Quadruplexer-Integrated Filtering Power Divider

CHI-FENG CHEN (Member, IEEE), KAI-WEI ZHOU, RUEI-YI CHEN, HSIN-YA TSENG, YI-HUA HE, WEN-JIE LI, AND WEI-CHENG JIANG

(Regular Paper)

Department of Electrical Engineering, Tunghai University, Taichung 40704, Taiwan

CORRESPONDING AUTHOR: Chi-Feng Chen (e-mail: cfchen@thu.edu.tw).

This work was supported by the Ministry of Science and Technology, Taiwan, under Grants MOST 109-2221-E-029-023 and MOST 109-2221-E-029-022.

ABSTRACT A compact quadruplexer with the functions of frequency division, frequency selection, and power splitting/combining is presented in this article. Four tri-mode stub-loaded resonators were adopted to construct the compact multifunctional quadruplexer with a third-order filtering response. The four-channel passbands of the quadruplexer were controlled and realized independently by using the distribution coupling configuration. The output coupling structure was designed to be symmetrical with equal power division for each channel. To achieve a satisfactory isolation performance, a resistor was loaded between the open ends of the output coupled lines for each channel. A microstrip multifunctional quadruplexer operating at 1.1, 1.44, 1.73, and 2.06 GHz was fabricated. The prototype circuit size of the multifunctional quadruplexer was only approximately 0.4 $\lambda_g \times 0.59\ \lambda_g$. Moreover, the output isolations were >27 dB within the entire frequency bands.

INDEX TERMS Bandpass filter (BPF), microstrip, quadruplexer, power divider (PD).

I. INTRODUCTION

Recent developments in radio frequency (RF) and microwave electronic systems have resulted in high demands on high-performance multifunctional circuits. Therefore, integrating a power divider (PD) and bandpass filter (BPF) into a single device, namely a filtering PD, is a popular research topic. Several filtering PDs using various design approaches have been proposed [1]–[7]. Furthermore, multi-band/multi-channel filtering PDs have been recently developed in [8]–[16].

In multiband and multichannel communication systems, multiplexers, BPFs, and PDs are essential components. For example, in quad-band applications, to achieve frequency division, frequency selection, and power division functions, a traditional solution is to connect a PD to each frequency channel of a quadruplexer comprising a five-port matching circuit and four different frequency BPFs (Fig. 1). Such an architecture requires nine circuits, which increases the system size and cost. To overcome this problem, another effective solution is to integrate these circuits into a single device as a multifunctional quadruplexer, which can achieve more than 50% size reduction compared to the cascaded configuration of a power-divider quadruplexer. Therefore, developing a multifunctional multiplexer is crucial for multiband and multichannel applications. However, few studies have designed such multifunctional multiplexers [17]–[20]. Moreover, the reported designs were presented only for dual-band/two-channel applications. In this article, a novel multifunctional

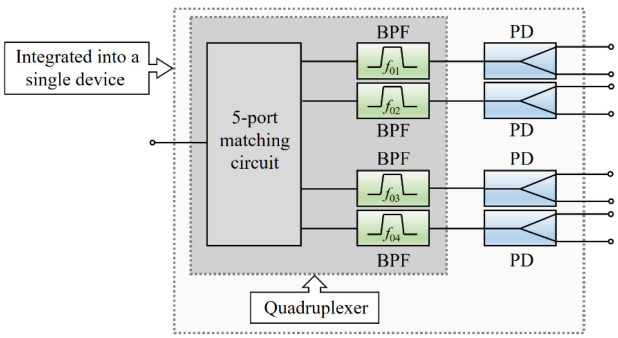

FIGURE. 1. Simplified architecture of a quadruplexer-integrated filtering PD.

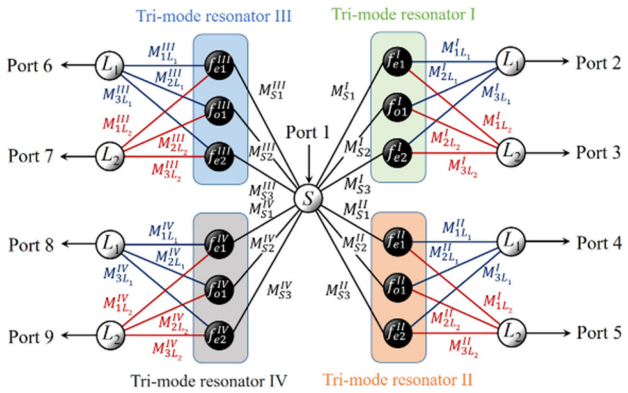

FIGURE. 2. Coupling scheme of the proposed quadruplexer-integrated filtering PD.

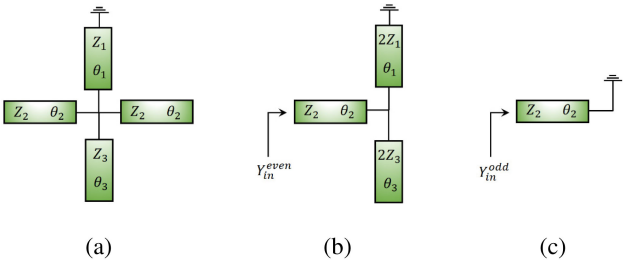

FIGURE. 3. (a) Circuit model of the tri-mode resonator. (b) Even-mode and (c) odd-mode equivalent circuit models.

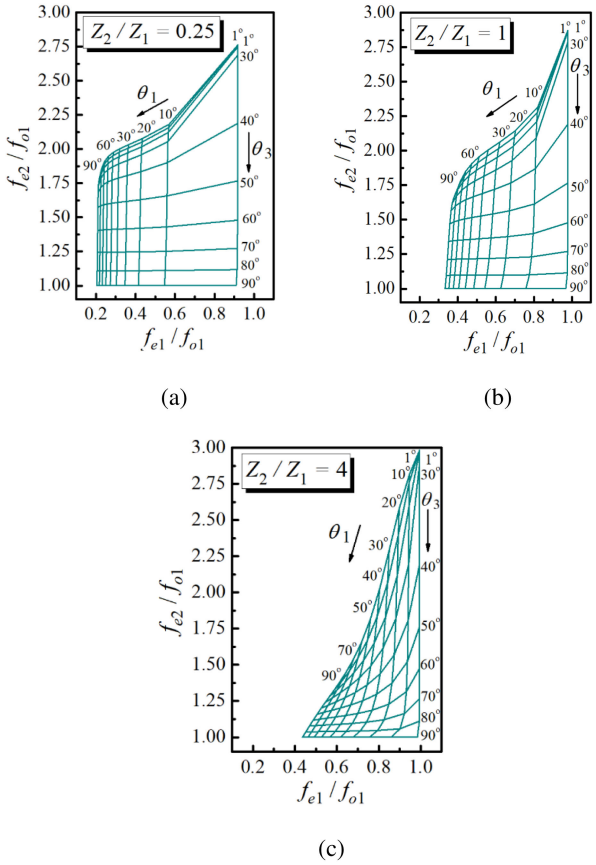

FIGURE. 4. f_{e2}/f_{o1} and f_{e1}/f_{o1} versus θ_1 and θ_4 with (a) $Z_2/Z_1 = 0.25$, (b) $Z_2/Z_1 = 1$, and (c) $Z_2/Z_1 = 4$.

quadruplexer is proposed. To the best of the authors' knowledge, this is the first time that a quadruplexer with the functions of frequency division, frequency selection, and power division has been implemented for quad-band/four-channel applications.

II. CIRCUIT DESIGN

Fig. 2 illustrates the coupling scheme of the proposed multifunctional quadruplexer, where each node represents a resonance mode; S and L denote the input and output ports, respectively. Four tri-mode resonators operating at different frequencies were used to construct the multifunctional quadruplexer. Here, f_{o1}^N, f_{e1}^N, and f_{e2}^N are the first odd-mode and the first two even-mode resonance frequencies of the tri-mode resonator, respectively, where the superscript represents the channel number (N = I, II, III, IV). The passband of channel N was formed by the resonance frequencies f_{o1}^N, f_{e1}^N, and f_{e2}^N. The signal was coupled from the input port (port 1) to each tri-mode resonator and finally coupled to the output ports: ports 2–9. The output coupling structure was designed to be symmetrical to ensure the signal was equally split into two output ports with the in-phase property for each channel. Note that, the isolation resistors are not included in Fig. 2 because the resistors had a negligible effect on the equal-split filtering response [6].

Fig. 3(a) displays the circuit model of the tri-mode stub-loaded resonator [21]–[23]. Because of the symmetric nature of the resonator, the resonance conditions can be analyzed by the even- and odd-mode equivalent circuits depicted in Fig. 3(b) and (c), respectively. For simplicity, we assumed that $Z_1 = Z_3$. By imposing $\mathrm{Im}[Y_{in}^{even}] = 0$ and $\mathrm{Im}[Y_{in}^{odd}] = 0$, the even- and odd-mode resonance conditions can be derived as follows:

$$Z_2(\cot\theta_1 - \tan\theta_3) = 2Z_1\tan\theta_2 \quad (1)$$

$$\cot\theta_2 = 0 \quad (2)$$

The relationships between the resonance frequencies (f_{e1}^N, f_{e2}^N, and f_{o1}^N) were obtained under resonant conditions and are plotted in Figs. 4(a), (b), and (c), respectively; the three resonance frequencies of the tri-mode resonator can be flexibly determined by adjusting its physical configuration.

A microstrip quadruplexer-integrated filtering PD was designed and validated. In this design, a Rogers RO4003C (ε_r = 3.55, h = 0.508 mm, and $\tan\delta$ = 0.0027) was used as the substrate. The targeted specifications are listed in Table I. According to given specifications, the coupling matrix can be synthesized as follows [24]:

TABLE 1. Specification

Channel	I	II	III	IV
CF (GHz)	1.1	1.44	1.73	2.06
BW (MHz)	60	80	75	100

CF: center frequency; BW: bandwidth

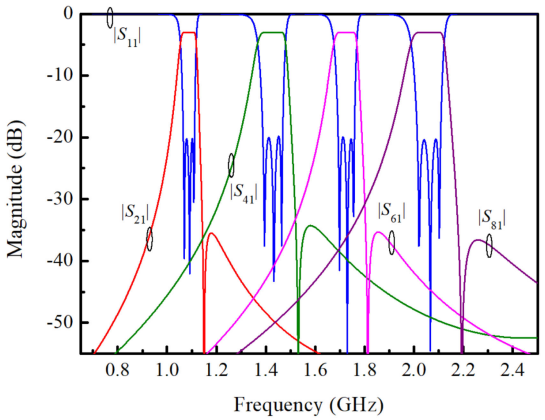

FIGURE. 5. Synthesized results of the proposed quadruplexer-integrated filtering PD.

$$[M]^N = \begin{bmatrix} 0 & 0.6 & -0.765 & 0.476 & 0 \\ 0.6 & 1.491 & 0 & 0 & 0.6 \\ -0.765 & 0 & -0.223 & 0 & 0.765 \\ 0.476 & 0 & 0 & -1.408 & 0.476 \\ 0 & 0.6 & 0.765 & 0.476 & 0 \end{bmatrix}$$

$$N = \mathrm{I},\ \mathrm{II},\ \mathrm{III},\ \mathrm{IV} \tag{3}$$

Fig. 5 shows the synthesized results of the quadruplexer-integrated filtering PD, without considering the loading effects of other channel filters, which meet the prescribed specifications. The configuration of the multifunctional quadruplexer is displayed in Fig. 6. To achieve compactness and reduce loading effect, two of the resonators (resonators II and IV) were firstly placed on the different sides near the open end of the input feeding line. Then, the other resonators (resonators I and III) were placed in the next available areas along the input feeding line with stronger current distributed at their resonance frequencies. By using the distributed coupling technique, the loading effects between channel passbands can be neglected [21], [25], [26]. Therefore, the four-channel passbands were independently designed. The desired resonance frequencies of each tri-mode resonator can be calculated as follows [27]:

$$f_n^N = \frac{f_0^N}{2} \cdot \left[\frac{-\Delta f^N}{f_0^n} M_{ii}^N + \sqrt{\left(\frac{\Delta f^N}{f_0^N} M_{ii}^N \right)^2 + 4} \right]$$

$$n = e1,\ o1, e2\ ;\ i = 1,\ 2,\ 3 \tag{4}$$

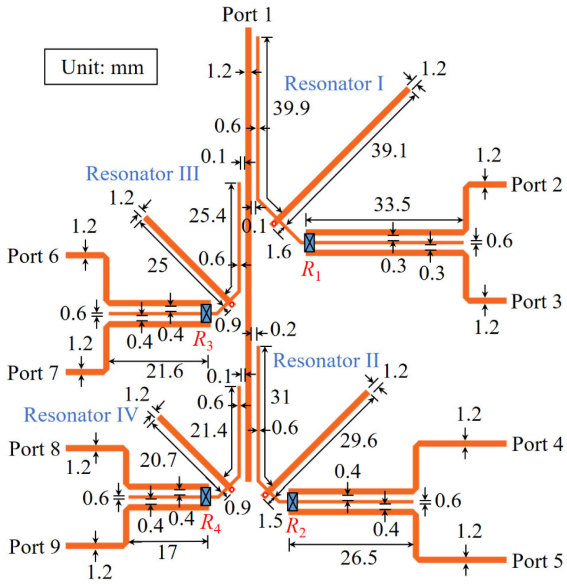

FIGURE. 6. Configuration of the proposed quadruplexer-integrated filtering PD.

where f_0^N and Δf^N are the center frequency and bandwidth of the passband for channel N, respectively. Subsequently, the physical configuration of each tri-mode resonator can be determined according to the derived frequencies $f_{e1}^I = 1.06$ GHz, $f_{o1}^I = 1.11$ GHz, $f_{e2}^I = 1.14$ GHz, $f_{e1}^{II} = 1.38$ GHz, $f_{o1}^{II} = 1.45$ GHz, $f_{e2}^{II} = 1.49$ GHz, $f_{e1}^{III} = 1.68$ GHz, $f_{o1}^{III} = 1.74$ GHz, $f_{e2}^{III} = 1.78$ GHz, $f_{e1}^{IV} = 1.99$ GHz, $f_{o1}^{IV} = 2.07$ GHz, and $f_{e2}^{IV} = 2.13$ GHz.

According to the specifications in Table I, the desired input external quality factors can be derived as follows [28]:

$$Q_{e,n}^N = \frac{f_0^N}{\Delta f^N \cdot M_{si}^2} \tag{5}$$

Notably, because the signal was equally split into two outputs for each channel, we obtain $M_{Si}^N = \sqrt{2} M_{iL}^N$. Thus, the output $Q_{e,n}^N$ was twice the value of the input $Q_{e,n}^N$. The desired input external quality factors result to be $Q_{e,e1}^I = 51$, $Q_{e,o1}^I = 31.3$, $Q_{e,e2}^I = 81.1$, $Q_{e,e1}^{II} = 50$, $Q_{e,o1}^{II} = 30.7$, $Q_{e,e2}^{II} = 79.6$, $Q_{e,e1}^{III} = 64.1$, $Q_{e,o1}^{III} = 39.4$, $Q_{e,e2}^{III} = 102$, $Q_{e,e1}^{IV} = 57.3$, $Q_{e,o1}^{IV} = 35.2$, and $Q_{e,e2}^{IV} = 91.1$. Meanwhile, the external quality factors can be extracted using the following equation [28]:

$$Q_e = \omega_0 \tau_d(\omega_0)/4 \tag{6}$$

where $\tau_d(\omega_0)$ is the group delay of S_{11} at resonance frequency ω_0. After that, the desired average value of external quality factors, i.e., $Q_e = (Q_{e,e1}^N + Q_{e,o1}^N + Q_{e,e2}^N)/3$, can be met by adjusting the gap, line width, and line length of the I/O coupled lines.

Finally, to improve isolation between the output ports, four resistors, namely R_1, R_2, R_3, and R_4, were connected at the open ends of the output coupled lines, as depicted in Fig. 6.

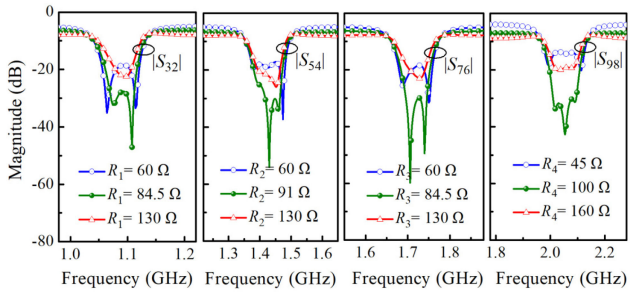

FIGURE. 7. Simulated isolation performances with varied R1, R2, R3, and R4.

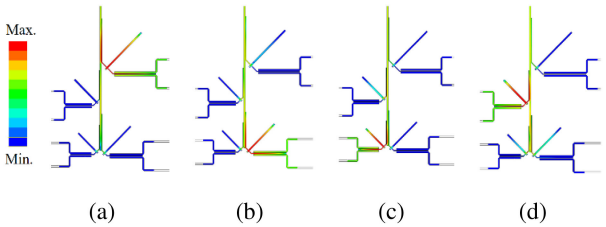

FIGURE. 8. Current distribution of the quadruplexer. (a) 1.1 GHz, (b) 1.44 GHz, (c) 1.73 GHz, and (d) 2.06 GHz.

Subsequently, the resistances of the four resistors were initially determined according to the matching condition of the odd-mode equivalent circuit [7] and optimized by appropriately tuning its value to achieve a satisfactory isolation performance by using an electromagnetic simulator. The simulated isolation performances with varied R_1, R_2, R_3, and R_4 are shown in Fig. 7. It is obvious that, the resistances can be chosen as $R_1 = 84.5\ \Omega$, $R_2 = 91\ \Omega$, $R_3 = 84.5\ \Omega$, and $R_4 = 100\ \Omega$ to achieve good isolation between output ports. Note that, the resistor can also be chosen to be connected at the other positions between the output coupled lines. Nevertheless, once the resistor location is changed, the resistance should be re-evaluated to achieve a satisfactory isolation performance.

The current distributions of the multifunctional quadruplexer at four-channel frequencies are displayed in Figs. 8(a), (b), (c), and (d). It is obviously found that the couplings between resonators were weak, which indicated that the loading effects between channel passbands were small. Thus, each passband of the quadruplexer can be individually realized.

III. EXPERIMENT AND MEASUREMENT

The physical dimensions of the multifunctional quadruplexer were determined according to the aforementioned deign procedure. The photograph of the fabricated circuit is displayed in Fig. 9. The overall circuit area was $0.4\ \lambda_g \times 0.59\ \lambda_g$, where λ_g is the guided wavelength at 1.1 GHz. Fig. 10 depicts the simulated and measured *S*-parameter of the proposed multifunctional quadruplexer. The multifunctional quadruplexer provided a third-order filtering function with equal power splitting for each channel. The measurement results revealed that the insertion losses at the channel passbands I, II, III, and

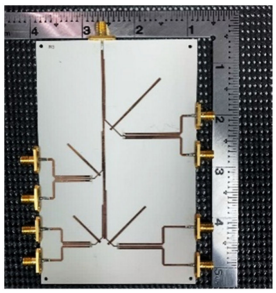

FIGURE. 9. Photograph of the fabricated circuit.

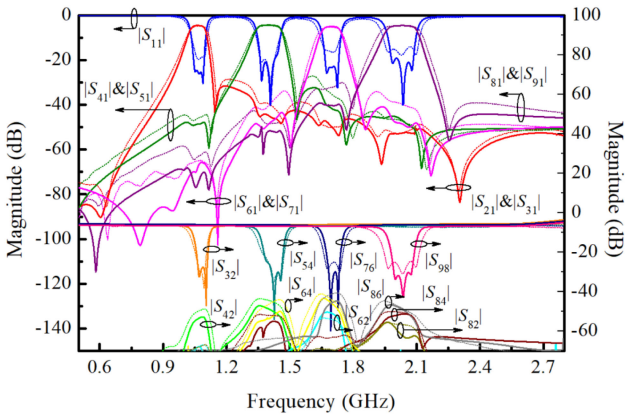

FIGURE. 10. Simulated and measured *S*-parameter of the proposed quadruplexer-integrated filtering PD. (Simulation: solid curves; measurement: dashed curves).

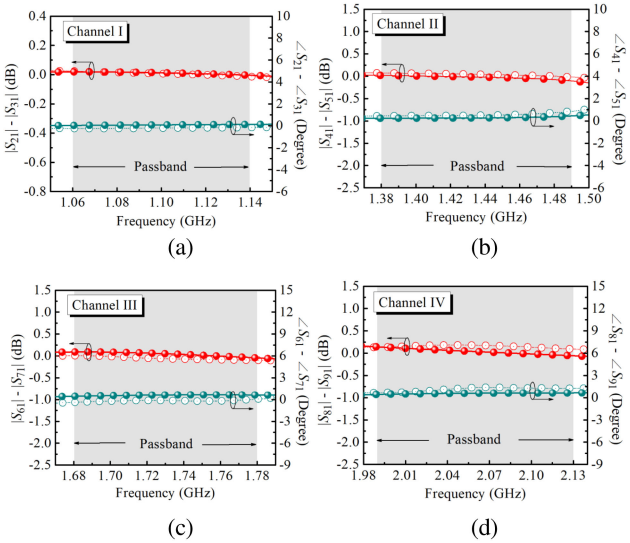

FIGURE. 11. Magnitude and phase imbalances for channels (a) I, (b) II, (c) III, and (d) IV. (Simulation: solid curves; measurement: dashed curves).

IV were approximately $(3 + 1.7)$, $(3 + 1.6)$, $(3 + 2.3)$, and $(3 + 1.7)$ dB, respectively, and the return losses were > 15 dB. The isolations between the output ports, namely S_{32}, S_{54}, S_{76}, and S_{98}, were > 27 dB within the operating bands. The port isolations between different channels were all > 40 dB. A

TABLE 2. Comparison of Various Multifunctional Multiplexers

	Ch	CF (GHz)	FO	IL (dB)	Iso (dB)	Size (λ_g^2)
This work	4	1.1, 1.44, 1.73, 2.06	3	4.7, 4.6, 5.3 4.7	> 27	0.23
[17]	2	1.77, 2.4	2	3.74, 3.95	> 20	> 0.3
[18]	2	2.5, 3	2	4.6, 4.9	> 21	0.2
[19]	2	1, 1.15	2	3.7, 3.8	> 28	0.26
[20]	2	1.8, 2.4	2	4.76, 4.75	> 20	> 0.8

Ch: channels; CF: center frequency; FO: filter order; IL: insertion loss; Iso: isolation

transmission zero (TZ) was generated at the upper side of each passband, which improved selectivity. The TZ was introduced when the stub loaded on the central plane of the resonator is at quarter-wavelength resonance [29], [30]. Furthermore, each channel filter can produce additional TZs at the passband frequencies of the other channels. This is due to the resonance of the tri-mode resonators of the other channels. As such, each of the tri-mode resonators behaves as a bandstop filter. The measured magnitude and phase imbalances were within 0.1 dB and 2°, respectively, as shown in Figs. 11(a), (b), (c), and (d).

Table II compares the proposed quadruplexer with other related circuits and indicates that the proposed quadruplexer has the most channel numbers/operating bands. In addition, the proposed quadruplexer is compact and exhibited high selectivity and in-band isolation.

IV. CONCLUSION

This study proposed a compact and high-performance multifunctional quadruplexer that can provide a third-order filtering function with equal power splitting for each channel. The design is flexible, and all channel passbands can be easily controlled. The proposed multifunctional quadruplexer is a promising device in RF and microwave applications because of its compact size ($0.4\ \lambda_g \times 0.59\ \lambda_g$), high selectivity (third-order filtering response with a TZ at the upper side of the passband), and high in-band isolation (> 27 dB).

REFERENCES

[1] Y. C. Li, Q. Xue, and X. Y. Zhang, "Single- and dual-band power dividers integrated with bandpass filters," *IEEE Microw. Wireless Compon. Lett.*, vol. 61, no. 1, pp. 69–71, Jan. 2013.

[2] C.-F. Chen, T.-Y. Huang, T.-M. Shen, and R.-B. Wu, "Design of miniaturized filtering power dividers for system-in-a-package," *IEEE Compon., Packag., Manuf. Technol.*, vol. 3, no. 10, pp. 1663–1672, Oct. 2013.

[3] W.-M. Chau, K.-W. Hsu, and W.-H. Tu, "Filter-based Wilkinson power divider," *IEEE Microw. Wireless Compon. Lett.*, vol. 24, no. 4, pp. 239–241, Apr. 2014.

[4] X. Wang, J. Wang, and G. Zhang, "Design of wideband filtering power divider with high selectivity and good isolation," *Electron. Lett.*, vol. 52, no. 16, pp. 1389–1391, Aug. 2016.

[5] G. Zhang, J. Wang, L. Zhu, and W. Wu, "Dual-mode filtering power divider with high passband selectivity and wide upper stopband," *IEEE Microw. Wireless Compon. Lett.*, vol. 27, no. 7, pp. 642–644, Jul. 2017.

[6] G. Zhang, X. Wang, J.-S. Hong, and J. Yang, "A high-performance dual-mode filtering power divider with simple layout," *IEEE Microw. Wireless Compon. Lett.*, vol. 28, no. 2, pp. 120–122, Feb. 2018.

[7] G. Zhang, Z. Qian, J. Yang, and J.-S. Hong, "Wideband four-way filtering power divider with sharp selectivity and high isolation using coshared multi-mode resonators," *IEEE Microw. Wireless Compon. Lett.*, vol. 29, no. 10, pp. 641–644, Oct. 2019.

[8] R. Gomez-Garcia, R. Loeches-Sanchez, D. Psychogiou, and D. Peroulis, "Single/multi-band Wilkinson-type power dividers with embedded transversal filtering sections and application to channelized filters," *IEEE Trans. Circuits Syst. I, Reg. Papers*, vol. 62, no. 6, pp. 1518–1527, Jun. 2015.

[9] D. Psychogiou, R. Gómez-García, A. C. Guyette, and D. Peroulis, "Reconfigurable single/multi-band filtering power divider based on quasi-bandpass sections," *IEEE Microw. Wireless Compon. Lett.*, vol. 26, no. 9, pp. 684–686, Sep. 2016.

[10] G. Zhang, J. Wang, L. Zhu, and W. Wu, "Dual-band filtering power divider with high selectivity and good isolation," *IEEE Microw. Wireless Compon. Lett.*, vol. 26, no. 10, pp. 774–776, Oct. 2016.

[11] Y. Wu, Z. Zhuang, G. Yan, Y. Liu, and Z. Ghassemlooy, "Generalized dual-band unequal filtering power divider with independently controllable bandwidth," *IEEE Trans. Microw. Theory Techn.*, vol. 65, no. 10, pp. 3838–3848, Oct. 2017.

[12] X. Wang, J. Wang, G. Zhang, J.-S. Hong, and W. Wu, "Dual-wideband filtering power divider with good isolation and high selectivity," *IEEE Microw. Wireless Compon. Lett.*, vol. 27, no. 12, pp. 1071–1073, Dec. 2017.

[13] G. Zhang, X. Wang, and J. Yang, "Dual-band microstrip filtering power divider based on one single multimode resonator," *IEEE Microw. Wireless Compon. Lett.*, vol. 28, no. 10, pp. 891–893, Oct. 2018.

[14] C. Zhu, J. Xu, and W. Wu, "Microstrip four-way reconfigurable single/dual/wideband filtering power divider with tunable frequency, bandwidth, and PDR," *IEEE Trans. Ind. Electron.*, vol. 65, no. 11, pp. 8840–8850, Nov. 2018.

[15] P. Wen *et al.*, "Dual-band filtering power divider using dual-resonance resonators with ultrawide stopband and good isolation," *IEEE Microw. Wireless Compon. Lett.*, vol. 29, no. 2, pp. 101–103, Feb. 2019.

[16] P.-L. Chi, Y.-M. Chen, and T. Yang, "Single-layer dual-band balanced substrate-integrated waveguide filtering power divider for 5G millimeter-wave applications," *IEEE Microw. Wireless Compon. Lett.*, vol. 30, no. 6, pp. 585–588, Jun. 2020.

[17] P.-H. Deng, W. Lo, B.-L. Chen, and C.-H. Lin, "Designs of diplexing power dividers," *IEEE Access*, vol. 6, pp. 3872–3881, Feb. 2018.

[18] G. Zhang, Z. Qian, and J. Yang, "Design of a compact microstrip power-divider diplexer with simple layout," *Electron. Lett.*, vol. 54, no. 16, pp. 1007–1009, Aug. 2018.

[19] C.-F. Chen, K.-W. Zhou, R.-Y. Chen, Z.-C. Wang, and H. Y.-H, "Design of a microstrip diplexer-integrated filtering power divider," *IEEE Access*, vol. 7, pp. 106514–106520, Aug. 2019.

[20] C.-H. Lin, P.-H. Deng, and W.-T. Chen, "Design of a microstrip diplexing filtering power divider," in *Asia-Pacific Microw. Conf. Dig.*, 2019, pp. 944–946.

[21] C.-F. Chen, T.-M. Shen, T.-Y. Huang, and R.-B. Wu, "Design of compact quadruplexer based on the tri-mode net-type resonators," *IEEE Microw. Wireless Compon. Lett.*, vol. 21, no. 10, pp. 534–536, Oct. 2011.

[22] Q. Li and Y. Zhang, "Six-channel diplexer with compact size and high isolation," *Electron. Lett.*, vol. 53, no. 17, pp. 1205–1207, Aug. 2017.

[23] Q. Li, Y. Zhang, and C.-T. M. Wu, "High-selectivity and miniaturized filtering Wilkinson power dividers integrated with multimode resonators," *IEEE Trans. Compon., Packag., Manuf. Technol.*, vol. 7, no. 12, pp. 1990–1997, Dec. 2017.

[24] R. J. Cameron, "Advanced coupling matrix synthesis techniques for microwave filters," *IEEE Trans. Microw. Theory Techn.*, vol. 51, no. 1, pp. 1–10, Jul. 2003.

[25] S.-J. Zeng, J.-Y. Wu, and W.-H. Tu, "Compact and high-isolation quadruplexer using distributed coupling technique," *IEEE Microw. Wireless Compon. Lett.*, vol. 21, no. 4, pp. 197–199, Apr. 2011.

[26] W.-H. Tu and C.-L. Wu, "Design of microstrip low-pass–bandpass multiplexers using distributed coupling technique," *IEEE Trans. Compon., Packag., Manuf. Technol.*, vol. 6, no. 11, pp. 1648–1655, Nov. 2016.
[27] G. Macchiarella, "Generalized coupling coefficient for filters with nonresonant nodes," *IEEE Microw. Wireless Compon. Lett.*, vol. 18, no. 12, pp. 773–775, Dec. 2008.
[28] J. S. Hong and M. J. Lancaster, *Microstrip Filter for RF/Microwave Application*. New York, NY, USA: Wiley, 2001.
[29] J. Xu, F. Liu, and Z.-Y. Feng, "Single-/dual-band bandpass filter-integrated single-pole double-throw switch using distributed coupling tri-mode resonators," *IEEE Trans. Microw. Theory Techn.*, vol. 68, no. 2, pp. 741–749, Feb. 2020.
[30] C. K. Liao, P. L. Chi, and C. Y. Chang, "Microstrip realization of generalized Chebyshev filters with box-like coupling schemes," *IEEE Trans. Microw. Theory Techn.*, vol. 55, no. 1, pp. 147–153, Jan. 2007.

CHI-FENG CHEN (Member, IEEE) received the M.S. degree in electrophysics from National Chiao Tung University, Hsinchu, Taiwan, in 2003, and the Ph.D. degree in communication engineering from National Taiwan University, Taipei, Taiwan, in 2006.

From 2008 to 2010, he was an RF Engineer with Compal Communications, Inc., Taipei, Taiwan, where he developed global system for mobile communication (GSM) and code division multiple access (CDMA) mobile phones. In April 2010, he joined the Graduate Institute of Communication Engineering, National Taiwan University, as a Postdoctoral Research Fellow. Since 2012, he has been a Faculty Member with the Department of Electrical Engineering, Tunghai University (THU), Taichung, Taiwan, where he is currently a Professor. His research interests include the design of microwave circuits and associated RF modules for microwave and millimeter-wave applications.

Dr. Chen was the recipient of the THU Excellent Teaching Award in 2020.

KAI-WEI ZHOU was born in Keelung, Taiwan, in 1996. He received the B.S. and M.S. degrees in electrical engineering from Tunghai University, Taichung, Taiwan, in 2019 and 2020, respectively. His current research interests include the design of microwave circuits.

RUEI-YI CHEN was born in Kaohsiung, Taiwan, in 1997. She is currently working toward the M.S. degree with the Department of Electrical Engineering, Tunghai University, Taichung, Taiwan. Her current research interests include the design of microwave circuits.

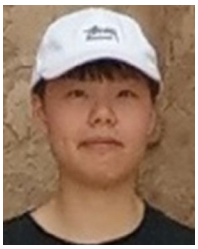

HSIN-YA TSENG was born in Tainan, Taiwan, in 1997. She is currently working toward the M.S. degree with the Department of Electrical Engineering, Tunghai University, Taichung, Taiwan. Her current research interests include the design of RF/microwave circuits.

YI-HUA HE was born in Taipei, Taiwan, in 1997. She is currently working toward the M.S. degree with the Department of Electrical Engineering, Tunghai University, Taichung, Taiwan. Her current research interests include the design of RF/microwave circuits.

WEN-JIE LE was born in Taoyuan, Taiwan, in 1998. She is currently working toward the M.S. degree with the Department of Electrical Engineering, Tunghai University, Taichung, Taiwan. Her current research interests include the design of RF/microwave circuits.

WEI-CHENG JIANG received the B.S. degree in computer science and information engineering and the M.S. degree in electro-optical and materials science from National Formosa University, Yunlin, Taiwan, in 2007 and 2009, respectively, and the Ph.D. degree in electric engineering from National Chung Cheng University, Chiayi, Taiwan, in 2013. He was a Postdoctoral Fellow with the Electrical Engineering Department, National Sun Yat-sen University, Kaohsiung, Taiwan. He was a Visiting Scholar with the Department of Electrical and Systems Engineering, Washington University in St. Louis, St. Louis, MO, USA. Since 2019, he has been an Assistant Professor with the Department of Electrical Engineering, Tunghai University, Taichung, Taiwan. His research interests include machine learning, multiagent systems, and intelligent control.